PAPER

Tribology study of lanthanum-treated graphene oxide thin film on silicon substrate

Zuhan Liu,[a] Da Shu,[a] Pengfei Li[a] and Xianhua Cheng*[ab]

Low friction coefficient and wear rate of components are crucial for nano-electromechanical-systems (NEMS). Herein, we have prepared carboxylated graphene oxide (GO) complexes with lanthanum on silicon substrate in order to form a two-dimensional self-assembled monolayer using 3-aminopropyl triethoxysilane (APTES) silane coupling agent (marked as APTES–GO–La). The chemical compositions, microstructures, and surface morphologies of samples were analysed by X-ray photoelectron spectroscopy (XPS), water contact angle (WCA), atomic force microscopy (AFM), and scanning electron microscopy (SEM). The tribology behaviour of the as-prepared thin films was tested by UMT-2 tribometer. Results show that GO sheets were successfully grafted on a silicon substrate and lanthanum was attached to a GO sheet by coordination reaction. The obtained APTES–GO–La film has a low friction coefficient and good wear-resistant properties. Its remarkable tribological properties are attributed to the strong bond of the film to the substrate and the special characteristics of the rare earth (RE) element and GO sheet. This film has potential applications in NEMS.

1. Introduction

Much progress has been made in regards to nano-electrome-chanical-systems (NEMS) technology in the past few years and many scientists and researchers have plunged into this regime for its potential applications in areas such as biological research and medical instruments, environmental energy converters, radio frequency and optical/IFR communication, *etc.*[1–3] Compared with the macroscopic engineering world, the microscopic length scale and high surface-area-to-volume ratio, characteristic of micro-electromechanical-systems, result in very high surface forces such as friction and adhesion, which seriously undermine the lifetime, reliability and performance of NEMS devices.[4,5] Improvement of the friction and wear behaviours of NEMS has become an urgent issue to tackle. Break-throughs in tribology performance of NEMS were brought about by preparation of a self-assembled monolayer (SAM), which could tremendously reduce the friction coefficient and increase wear-resistance because of its strong head group–substrate binding, dense packing of hydrocarbon chains, and low surface free energy.[6,7] It should be noted that both molecular properties and the cross linking interactions between molecular chains have a significant effect on friction and wear performance of SAM films.[8] Based on this, we have prepared GO self-assembled composite thin films, aiming to further improve the friction and wear behaviours of the silicon substrate.

Graphene, a two-dimensional (2D) honeycomb lattice, has led to much excitement since it was first reported in 2004[9] because of its interesting characteristics, such as extraordinary thermal, mechanical, and electrical properties, *etc.*[10–16] Potential applications of graphene in NEMS have been actively pursued since the theoretical thickness of single-layered graphene is only 0.34 nm, which is exactly suitable for NEMS. Filleter *et al.*[17] found that graphene films exhibit frictional properties rather similar to those of bulk graphite and could be used as low-friction anti-wear coatings on silicon carbide surfaces. Jiangnan Zhang *et al.*[18] studied nanoscale frictional characteristics of three types of chemically treated graphene nanoribbons and found that the measured friction differences are attributed to the surface reactivity and hydrophilicity differences induced by different chemical functionalization schemes. However, a stable graphene film on a silicon substrate is difficult to prepare by a common solution process due to the lack of active functional groups on its surface. The existence of hydroxyl groups, carboxyl groups, and epoxy groups on GO sheets makes this possible,[19] although these active oxygenous groups can have a negative impact resulting in a decrease of friction and wear performance. J. Ou has studied the reduced graphene oxide (RGO) film and self-assembled graphene oxide octadecyltri-chlorosilane (APTES–GO–OTS) trilayer film, which can dramat-ically reduce the influence of these active groups on friction and wear properties.[20,21] The downside of these two methods is that the preparation of an RGO film requires relatively complex experimental conditions and the preparation of an

[a]*School of Mechanical and Power Energy Engineering, Shanghai Jiao Tong University, Shanghai 200240, PR China. E-mail: xhcheng@sjtu.edu.cn; Fax: +86 021 2136203; Tel: +86 021 36206366*

[b]*State Key Laboratory of Solid Lubrication, Lanzhou Institute of Chemical Physics, Chinese Academy of Sciences, Lanzhou 730000, PR China*

APTES–GO–OTS film, to some extent, increases the thickness of the thin film. It is well known that the small clearances associated with NEMS are only on the order of a few molecules thick.[22] Furthermore, the top level of the APTES–GO–OTS film may affect the graphene to give full play to friction reduction and wear resistance properties since OTS covers the graphene sheets. Given the above reasons, we attempted to make use of rare earths (REs) to improve the ability of APTES–GO composite thin film.

Rare earths (REs) have been widely applied in many fields such as optics, medicine, chemistry and magnetism for their special 4f electron shell structure.[23–28] It is little known that REs can improve tribology behaviour with their superior friction-reducing and wear-resistant abilities. In our previous research, we prepared RE-silane SAM films on silicon wafer surfaces. Results showed that the application of REs to those SAM films greatly improved their tribology performance.[29,30]

In this paper, we prepared APTES–GO–La thin film, and analyzed its structure by means of X-ray photoelectron spectroscopy (XPS), water contact angle (WCA), *etc.* In addition, tribological performance of samples was investigated and their friction and wear mechanisms were discussed. Owing to the self-lubricating and outstanding mechanical properties of GO and good tribological behaviour of REs, the prepared APTES–GO–La film has remarkable tribological performance. Many researchers have studied tribological properties of different SAMs. However, to our knowledge, the attempt to assemble APTES–GO–La thin film has not been made. This study is helpful to the design and selection of appropriate thin films for NEMS.

2.   Experimental details

2.1.   Materials

Expandable graphite, purchased from Nanjing XFNANO Materials Tech Co., Ltd, was used to prepare GO. 3-Aminopropyl triethoxysilane coupling agent (APTES, 99%, $\rho = 0.942 \text{ g mL}^{-1}$), lanthanum trichloride ($LaCl_3$) and chloroacetic acid ($Cl–CH_2–COOH$) were acquired from Aldrich Chemical Co., Inc. Silicon wafer (100) obtained from Zhejiang Cubic Crystalline Silicon Materials Co., Ltd was cut into the size of 5 mm × 10 mm to be used as substrate for the SAM film transfer. All other reagents were of analytical grade and used as received. Deionized water was used throughout the whole experiment.

2.2.   Preparation of GO–COOH solution

GO was prepared by a modified Hummers method.[31–33] Briefly, expandable graphite (1 g) instead of graphite flakes, to ensure more uniform oxidization, was soaked in concentrated H_2SO_4 (23 mL) for 8 h to effect intercalation. After addition of $KMnO_4$ (3 g) as oxidizing agent, the mixture was stirred at 40 °C for 30 min to get fully and uniformly oxidized graphite. Subsequently, distilled water (46 mL) was slowly added and the mixture was kept at 100 °C for 30 min. Then, the mixture was washed with distilled water (140 mL) and 30% H_2O_2 solution (10 mL). The resulting mixture was repeatedly centrifuged and filtrated until

pH was approximately 7 and SO_4^{2-} anions could not be detected.[34] After the products were sonicated for 2 h, the resulting GO particles were mostly single-layered according to atomic force microscopy (AFM) characterization.

The obtained GO was treated with chloroacetic acid to allow the transformation of hydroxyl and epoxy groups to carboxyl groups. A scheme of the carboxylated GO preparation process is shown in Fig. 1(a). The obtained GO was sonicated for 1 h with NaOH alkaline solution to attain GO colloidal solution. The obtained GO colloidal solution was sonicated for another 1–3 h and excess chloroacetic acid was added simultaneously. Then the product was purified and thoroughly washed with water until the suspension reached approximately pH 7. Thus, a homogeneous carboxylated graphene oxide suspension was obtained and marked as GO–COOH.[26,34]

2.3.   Fabrication of multilayer film

A scheme for the preparation of different kinds of films is shown in Fig. 1(b and c). Prior to the deposition of SAMs, silicon wafers were cleaned ultrasonically with absolute ethanol and deionized water in turn to remove other ions and molecules physically absorbed on the surface. Then, the silicon wafers were immersed in piranha solution (a mixture of 3 : 1 (v/v) 98% H_2SO_4 and 30% H_2O_2) at 90 °C for 30 min to make hydroxyl radicals on the surface, followed by a repeated washing with deionized water. After that, the obtained silicon wafers were dipped into fresh APTES solution (0.5 mM; the solvent is a mixture of acetone and water, with a volume ratio of 5 : 1) at ambient temperature for 30 minutes. Subsequently, the wafers were rinsed with deionized water and dried for 1 h at 120 °C under nitrogen atmosphere. At this point, APTES-SAM was obtained and, on this basis, GO was successfully grafted onto the silicon substrate by keeping the APTES-SAM films in the surface-modified GO–COOH aqueous solution (0.3 mg L^{-1}) at 80 °C for 12 h, then cleaning them in deionized water and drying them in nitrogen (see Fig. 1(b)). This film, covered homogenously with carboxylated graphene oxide, was coded APTES–GO. Finally, the APTES–GO films were immersed in RE ethanol solution (2 mM) at 90 °C for 12 h. The resulting products, thoroughly rinsed with deionized water and dried under nitrogen atmosphere, were marked as APTES–GO–La (see Fig. 1(c)).

For comparison, we prepared APTES–RGO film by reducing APTES–GO at 200 °C for 2 h at a heating rate of 1 °C min^{-1} under the protection of argon gas.[35,36]

2.4.   Experimental apparatus and measurements

Morphological properties of APTES–GO–La were investigated by a NanoScope IIIa AFM (produced by Shimadzu Corporation, Japan) in tapping mode, as it is crucial to study the morphology in the research of the self-assembly technique. SEM (Model Leica, Stereoscan 440) was employed to observe the surface microstructure of the samples after being sputtered with a thin gold coating.

XPS is an ideal diagnostic tool to assess the chemical state of elements. In this paper, XPS analysis was conducted on a
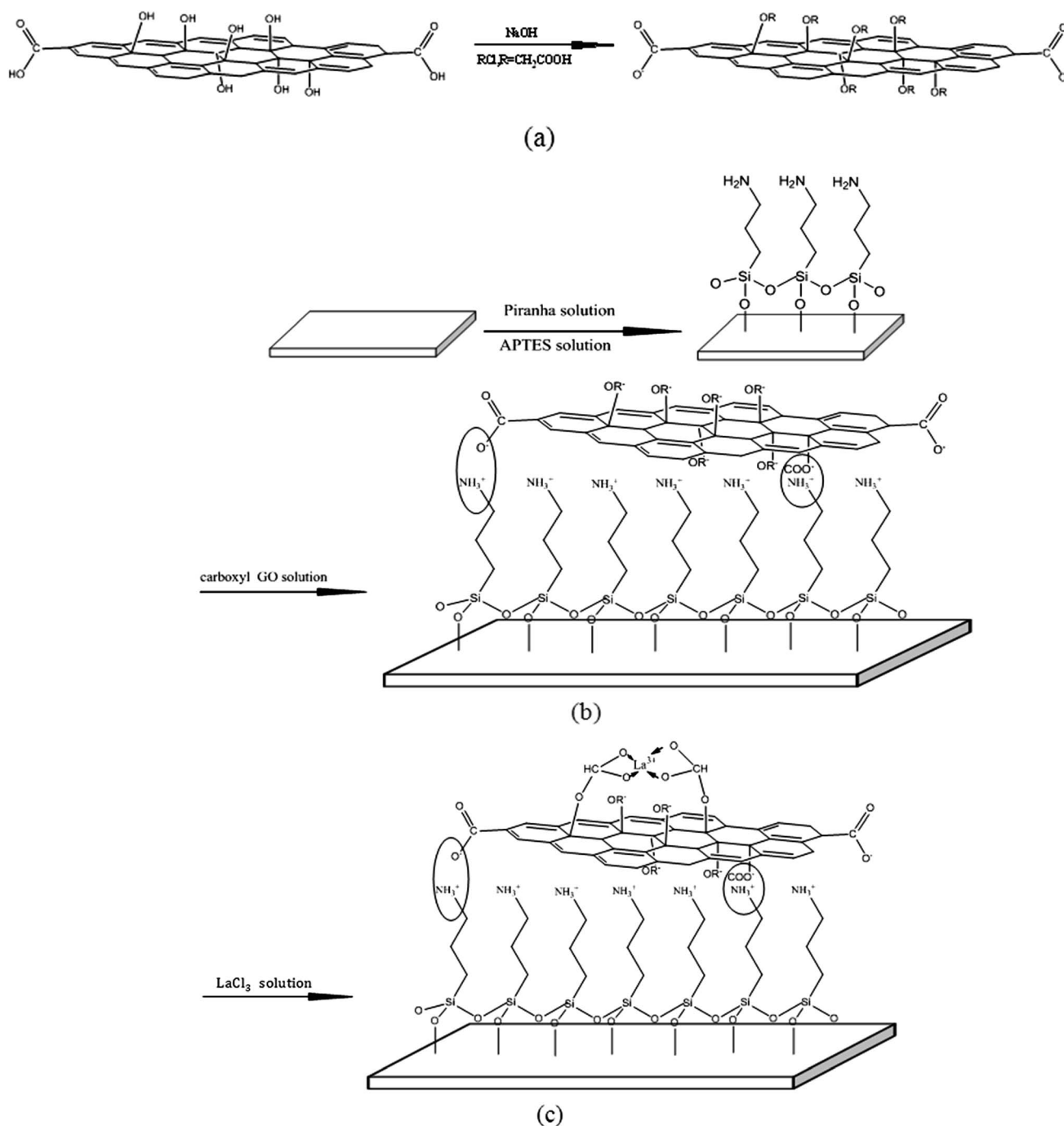
Fig. 1 Schematic diagram illustrates the preparation of samples: (a) carboxy functionalized GO sheet (GO–COOH), (b) APTES-SAM film and APTES–GO film, (c) APTES–GO–La film.

PHI-5702 XPS system ($h\nu = 1253.6$ eV) at a pass energy of 29.4 eV, using monochromatic AlKα irradiation. The resolution of the C 1s binding energy is about ±0.3 eV with the binding energy of contaminated carbon (C 1s: 284.6 eV) as the reference.

The static WCA of the samples was measured on the OCA-20 measurement apparatus (Data Physics Instruments GmbH) at ambient conditions (23 °C) with relative humidity 40%. Typically, 10 μL droplets of deionized water were used to make contact angle measurements. Contact angle was measured on five different spots on the samples, and all results on each sample were averaged.

The tribological properties of different thin films were tested on a UMT-2 tribometer in a ball-on-plate contact mode under ambient conditions (relative humidity 40%). The matching part was a GCr15 steel ball of diameter 3 mm with surface roughness (Ra) 0.02 μm. The sliding velocity and stroke were 5 mm s^{-1} and 5 mm. The normal load was set at 0.1 N and 0.2 N. The friction coefficient and running time were recorded automatically. The

friction coefficient remained relatively stable with slight fluctuation during the whole testing process. When the friction coefficient suddenly increased to a high value (>0.5), it indicated that the film had failed. The corresponding sliding times were equivalent to the wear life of samples. Replicate tests were performed at least three times at different spots for each sample and the friction coefficient and wear life were the average of the three results.

3. Results and discussion

3.1. SEM and AFM analysis

Fig. 1 illustrates the assembling mechanism of the APTES–GO film. The existence of abundant polar oxygenous groups (such as carboxyl functionalized groups) enables GO to dissolve well in aqueous solution and react with amino groups of APTES molecules.[34,37] By means of this amidation reaction, GO sheets are chemically combined with APTES by covalent bonding, and hence, assemble on the surface of the silicon wafers.[20]

The single-sheet nature of the graphene oxide obtained is confirmed by atomic force microscopy (AFM, Fig. 2(a and b)). As shown in Fig. 2(a), a single-layer GO sheet and overlapping sheet can be observed on the surface of the silicon substrate. The thickness of the GO sheet obtained is about 1.3 nm, which is a little greater than the theoretical thickness of the exfoliated graphene oxide (about 1.2 nm). This can be attributed to the intrinsic out-of-plane deformation of graphene[38,39] as well as to the instrumental offset arising from different interaction forces between the AFM probe, the graphene oxide sheet, and the substrate.[40] Generally, this thickness value is consistent with others reported in previous studies.[41–43] From the SEM images of APTES–GO film (Fig. 2(c)), we can observe that the graphene oxide is uniformly distributed on the substrate surface. This is ascribed to the fact that the carboxylated GO with abundant carboxyl groups can dissolve well in water.

3.2. XPS analysis

The presence of APTES–GO–La film on silicon substrate was substantiated by XPS measurements. As shown in Fig. 3(b), the signal at 288.9 eV corresponds to the O–C=O bond, indicating that GO has been successfully assembled on the APTES-SAM film, while the signals at 285.8 eV and 284.6 eV correspond to the C–O bond and the C–C bond, respectively.[20] Compared to APTES–GO film, there are some new peaks appearing at 800 eV

to 1000 eV in APTES–GO–La film, suggesting that La has been introduced in the APTES–GO film. The high-resolution spectra of the La 3d signal seen in Fig. 3(c) shows four peaks, whose binding energies are 835.25 eV, 838.75 eV, 852.125 eV and 855.625 eV, respectively. Compared with our early test data, the characteristic peak values of $LaCl_3$ are 853.0 eV and 856.7 eV. Thus, a rational inference can be made that the La really reacts with carboxylate ions. Fig. 3(d) is a schematic diagram of the probable coordination reaction. After the APTES–GO film is dipped into RE solution, a large number of (COO^-) anions generated from COOH on the surface of GO become the active sites for La^{3+}, then a coordination reaction occurs between COO^- anions and La^{3+} ions.[26] It is worth mentioning that the coordination reaction may occur at the edge of different GO sheets (as Fig. 3(d)-I shows), which can enhance the bonding force of lateral combination. Also, it may occur on the GO sheet surface (as Fig. 3(d)-II shows), which can reduce the surface free energy.

3.3. Water contact angle analysis

Water contact angle (WCA)[44] is an easy and effective way to characterize the properties of a given surface including surface free energy, hydrophobicity, and hydrophilicity. We performed the WCA measurement of hydroxylated Si, APTES-SAM, APTES–GO, APTES–RGO, and APTES–GO–La films. As Table 1 shows, the hydroxylated silicon substrate, with contact angle less than 10°, is hydrophilic, indicating that the silicon substrate was thoroughly hydroxylated after treatment in piranha solution, which increased the surface free energy. By contrast, the contact angles of APTES-SAM film and APTES–GO film increased to 51.0° and 53.8°, respectively. It may be concluded that the silicon substrate had been successfully coated with APTES-SAM film and APTES–GO film, whose moderately polar groups such as oxygenous and amine groups led to the reduction of surface energy.[45,46] Table 1 also gives the contact angle of APTES–RGO (80.5°). The sharp increase of contact angle is due to the disappearance of oxygenous functional groups on GO sheets caused by thermal reduction. The contact angle of APTES–GO–La film is 78.3°, which is fairly close to the contact angle of APTES–RGO film, thus, demonstrating that lanthanum ions had successfully deposited on the APTES–GO films. It can be explained by taking into account the fact that lanthanum ions can form ionic bonds with several nearby COO^- anions on GO,
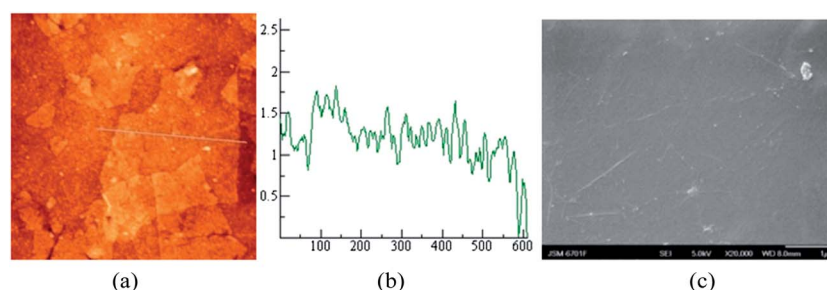

Fig. 2 (a) AFM image of Si–GO. (b) The thickness value of GO (corresponding to the mark in (a)). (c) SEM image of APTES–GO film.
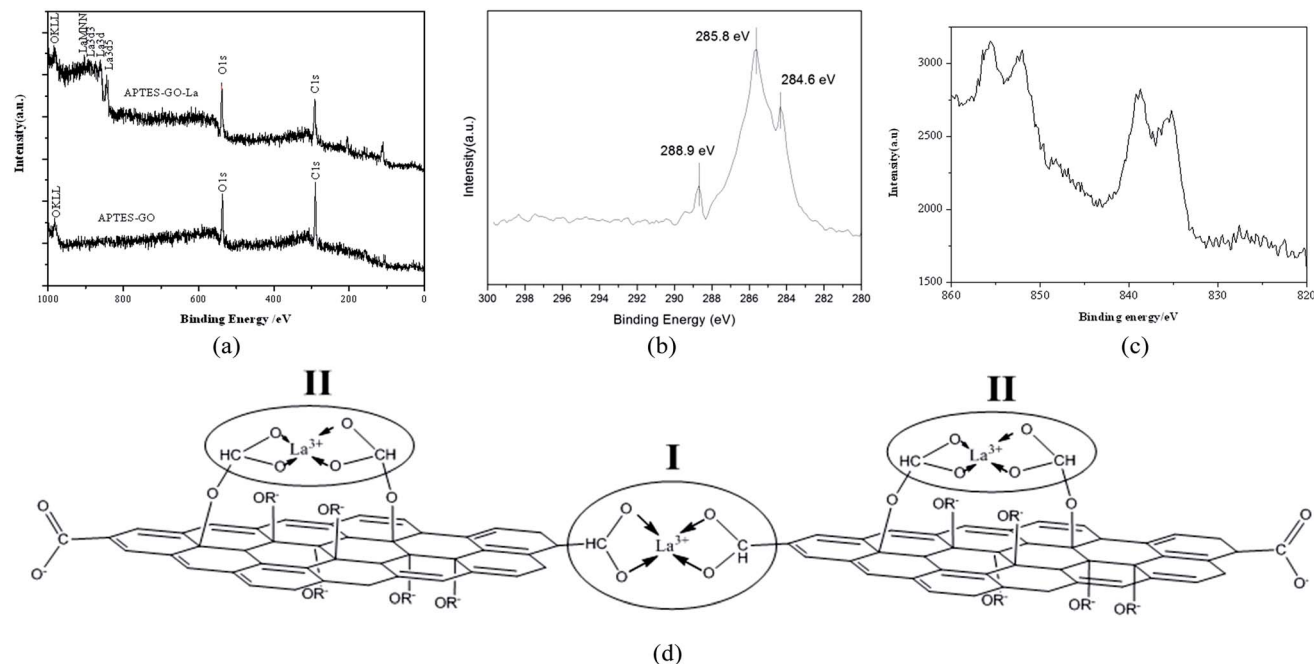
Fig. 3 (a) XPS spectra of APTES−GO−La thin film. (b) High-resolution XPS spectra of C 1s on APTES−GO−La thin film. (c) High-resolution XPS spectra of La 3d on APTES−GO−La thin film. (d) Probable coordination reaction.

Table 1 Water contact angle of various samples

Samples	Si (hydroxylated)	APTES-SAM	APTES−GO	APTES−RGO	APTES−GO−La
WCA (deg)	<10	51.0 ± 2.6	53.8 ± 1.4	80.5 ± 1.3	78.3 ± 2.5

or ligand bonds with oxygen on APTES, making the hydrophilic group COO^- immobile on the surface and arranged in such a way that they are not exposed outward, which will reduce the number per unit area of hydrogen bond formation. It should be kept in mind that, for APTES−GO film, the high surface free energy results from hydrogen bond formation, where the electron-donor sites come from the COO^- groups and the electron-acceptor interaction originates from the polar probe liquid molecules, which are water. Therefore, it is reasonable to conclude that APTES−GO−La film has a lower surface free energy than APTES−GO film when its density of hydrogen bonds is smaller. There could be several other reasons for this, such as changes in the nanoscale roughness due to surface functionalization,[47] flexibility and rotational mobility of functional groups,[48] and conformational changes in the functional groups.[49] To find a clear explanation, further studies are needed.

3.4. Tribological behaviour of samples

The friction coefficient and wear life of the prepared samples were obtained on a UMT-2 friction tester. Fig. 4 shows the variation of frictional coefficient of different SAMs as a function of sliding time. It can be seen, from Fig. 4(a), that APTES-SAM recorded a high friction coefficient around 0.36 and short wear life less than 60 s. APTES−GO film (Fig. 4(b)) shows better tribological properties with friction coefficient 0.21 and wear life 1320 s. This can be ascribed to the excellent mechanical and self-lubricating properties of GO, which improve the tribological performance of APTES−GO film.[20,21] The friction coefficient of APTES−RGO film (Fig. 5(c)) was 0.22, little changed from the APTES−GO film, while the wear life has a remarkable improvement (>3600 s). This significant change is due to a lower surface free energy than APTES−GO film. Low surface free energy can reduce adhesive bonds of the solid contact surface, therefore, friction coefficient values of SAMs having lower surface energy are expected to be lower and wear life accordingly longer.[20,50] The friction coefficient value of APTES−GO−La film shown in Fig. 4(d) is 0.13, which is the best among APTES-SAM, APTES−GO, APTES−RGO and APTES−GO−La films. Furthermore, the wear life is longer than 3600 s, equal to that of APTES−RGO film. This is mainly because lanthanum ions introduced in APTES−GO−La films not only greatly decrease the surface free energy, but also enhance some mechanical properties, which determine the resistance to permanent plastic deformation of the materials and improve the tribological properties.[51] Lanthanum ions can form ionic bonds with COO^- anions on GO, or ligand bonds with oxygen on APTES and acylamino groups. Both of these can increase the density of chemical bonds, thereby, increasing the shear strength and the hardness of the films.[52] It is found,
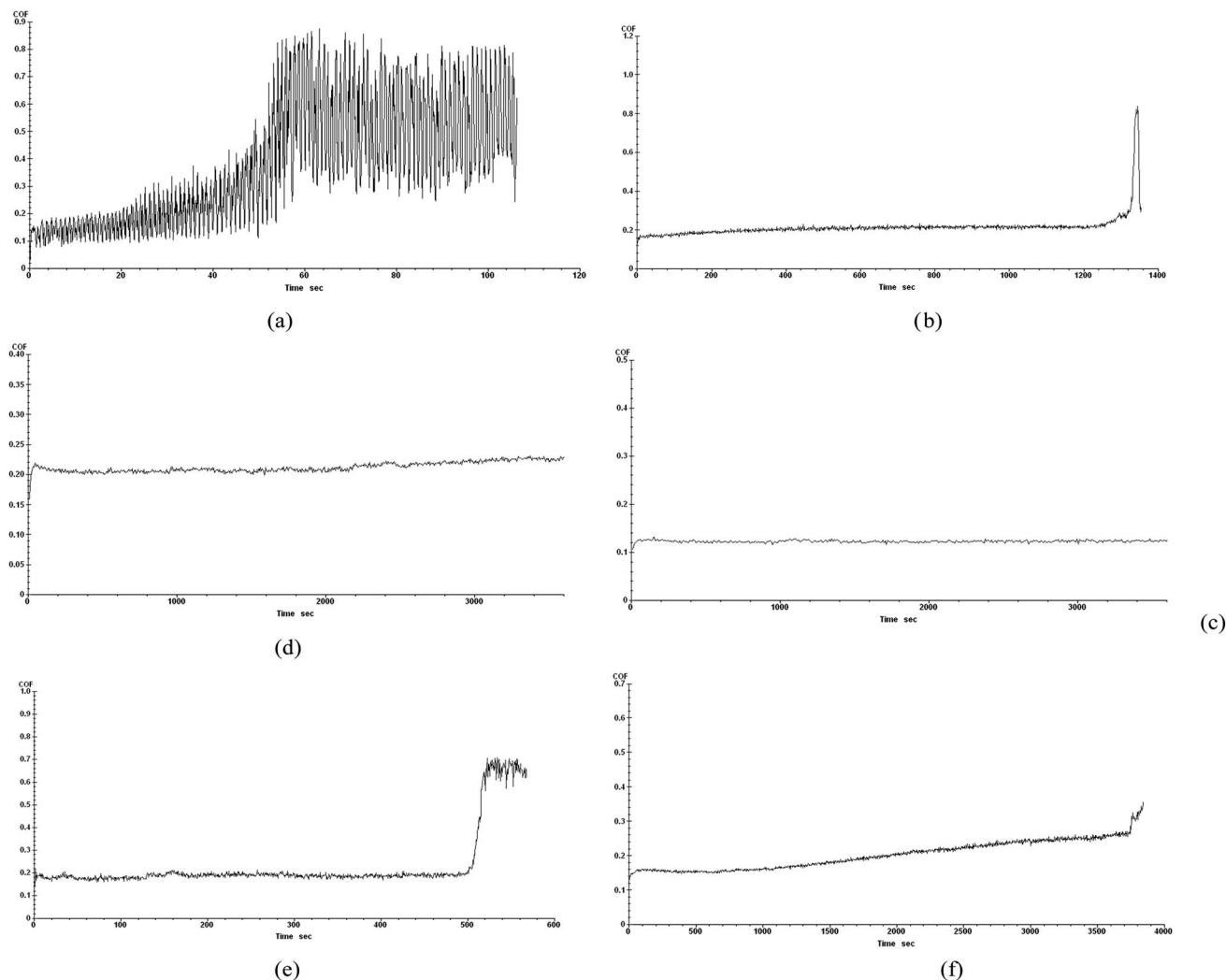
Fig. 4 Friction coefficient of samples as a function of sliding time for various samples under different loads at a sliding frequency of 1 Hz: (a) APTES–SAM (0.1 N), (b) APTES–GO (0.1 N), (c) APTES–RGO (0.1 N), (d) APTES–GO–La (0.1 N), (e) APTES–RGO (0.2 N), (f) APTES–GO–La (0.2 N).

qualitatively, that low friction coefficients are found for sliding materials with low surface energy/hardness ratios in the friction field. The hard films exhibit better mechanical and wear properties. Regardless of how they are formed, solid surfaces generally contain surface irregularities. The contact between two nominally flat surfaces occurs at discrete contact points as a result of surface roughness. The sum of the areas of all the contact points constitutes the real area of contact and deformation often occurs at these points. This deformation is usually plastic for a softer material at heavy loads, which can cause plastic flow deformation and a ploughing effect during friction and increase the actual contact area with increase in the contact
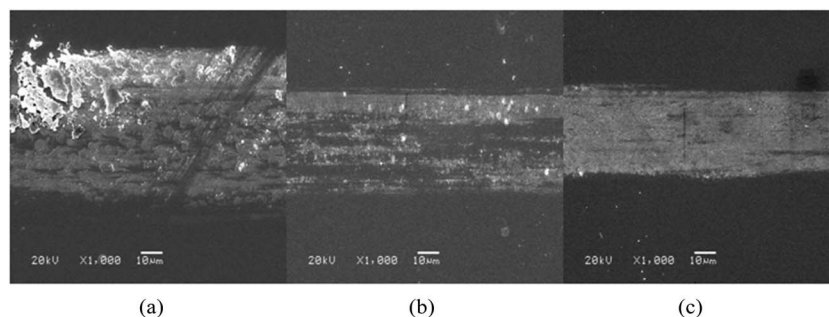

Fig. 5 SEM images of wear track of (a) APTES–GO film, (b) APTES–RGO film and (c) APTES–GO–La film.

time, finally giving rise to an increase of adhesion. That is why APTES–GO–La films have a lower friction coefficient value, though having a smaller water contact angle than APTES–RGO films. Fig. 4(e and f) shows the tribological performance of APTES–RGO film and APTES–GO–La film under a normal load of 0.2 N at sliding frequency 1 Hz. Fig. 4 (e and f) shows that APTES–GO–La film exhibits a frictional coefficient close to that of APTES–RGO films, but has a longer wear life (3750 s). This peculiar phenomenon can also be ascribed to lanthanum ions. The lanthanum ions intruded in the defects of the APTES–GO–La films can form strong chemical affinity with carbon, oxygen, nitrogen or hydrogen on APTES and GO, or form ionic bonds with COO^- anions. These interdigitations will greatly reinforce the bonding force between APTES–GO–La films and the silicon surface to withstand the large shear due to friction force under heavy loads, in contrast with APTES–RGO films.

To further understand the influence of lanthanum ions on the microscale friction behaviour, we investigated the wear tracks of APTES–GO film, APTES–RGO film, and APTES–GO–La film using SEM after the friction test under load 0.1 N and at sliding frequency 1 Hz. Their wear tracks reveal why APTES–GO–La film has the best anti-wear properties. APTES–GO–La film has the most homogeneous wear scar (Fig. 5(c)) among the three SAM films within the same time frame. Having good shear resistance and hardness, this uniform and smooth film reduced the apparent areas of contact and the number of particles trapped at the interface, thus, minimized the 'ploughing' contribution to the friction force. The APTES–RGO film has some shot-like particles around the wear spot, which would cause abrasive wear and exacerbate the wear. The APTES–GO film even has a large amount of abrasive dust piling up in the wear scar which is caused by the exfoliation and agglomeration of GO sheets. Although the deoxygenation of GO decreases the surface activity of graphene sheets and the friction coefficient, the interface force between adjacent APTES–RGO film is also weakened. Thus, some APTES–RGO films not firmly fixed on silicon substrate or bonding loosely to neighbours become wear debris, stacking on the sliding area and aggravating the roughness, which, in return, produces more wear debris. In contrast, the introduction of lanthanum in the APTES–GO–La film not only reduces the surface free energy, but also enhances the strength between adjacent GOs. Therefore, it makes much more sense why APTES–GO–La film has the best tribological properties.

The friction and wear mechanisms for APTES–RGO film and APTES–GO–La film can be illustrated by a simple schematic diagram (Fig. 6(a and b)). For APTES–RGO film, the silane molecules connected with GO sheets are divided into small discontinuous pieces under the normal load. Therefore, the steel ball needs to overcome the lateral van der Waals force between alkyl chains during the course of friction. However, for APTES–GO–La film, these discontinuous pieces can cross link with each other by chemical bonding to form a whole large film through lanthanum ions (see Fig. 6(b)). The cross linkage can uniformly disperse the lateral friction force on films and, thus, enhance the wear resistance properties of the APTES–GO–La film.

4.　Conclusions

In this work, graphene oxide was covalently assembled on a silicon substrate *via* amidation reaction between carboxyl on carboxylated GO and the amino groups of APTES molecules. APTES–GO films had a low friction coefficient (around 0.21), owing to the excellent mechanical and self-lubricating properties of GO. With the introduction of lanthanum ions, APTES–GO–La films exhibited excellent friction reduction and wear resistance properties, under relatively high applied load, in comparison with APTES–RGO films. The superior tribology performance of APTES–GO–La films was attributed to the fact that the coordination chemistry reaction between La and carboxyl groups decreased surface free energy and improved the lateral cross linking binding force. The APTES–GO–La film prepared by this method can serve as a low-friction anti-wear coating in NEMS. Although the proposed approach is based on silicon wafers, it has a potential application in many other substrates, such as glass, mica, and metal oxides and so on.

Acknowledgements

Fig. 6 Schematic diagram of (a) APTES–RGO film and (b) APTES–GO–La film.

Notes and references

1 K. Komvopoulos, *Wear*, 1996, **200**, 305–327.

2 S. M. Spearing, *Acta Mater.*, 2000, **48**, 179–196.

3 J. A. Williams and H. R. Le, *J. Phys. D: Appl. Phys.*, 2006, **39**, R201–R214.

4 B. Bhushan, *Tribology Issues and Opportunities in MEMS*, Kluwer Academic, Dordrecht, 1998.

5 R. Maboudian and C. Carraro, *Annu. Rev. Phys. Chem.*, 2004, **55**, 35–54.

6 F. Schreiber, *J. Phys.: Condens. Matter*, 2004, **16**, R881–R900.

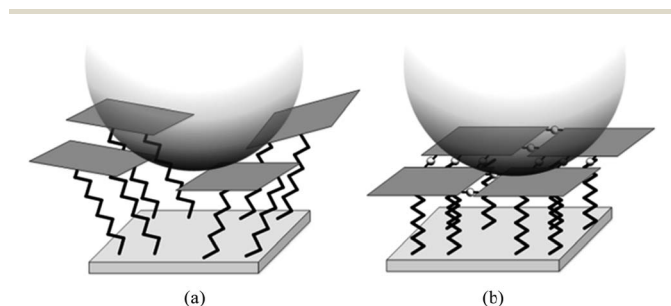7 H. Wang, Y. Zhu, X. Feng and X. Lu, *Wear*, 2010, **269**, 139–144.

8 R. Bautista, N. Hartmann and E. Hasselbrink, *Langmuir*, 2003, **19**, 6590–6593.

9 K. S. Novoselov, A. K. Geim, S. V. Morozov, D. Jiang, Y. Zhang, S. V. Dubonos, I. V. Grigorieva and A. A. Firsov, *Science*, 2004, **306**, 666–669.

10 V. C. Tung, M. J. Allen and R. B. Kaner, *Chem. Rev.*, 2010, **110**, 132–145.

11 Z. S. F. Bonaccorso, T. Hasan and A. C. Ferrari, *Nat. Photonics*, 2010, **4**, 611–612.

12 J. W. W. P. K. Mullen, *Chem. Rev.*, 2007, **107**, 718–747.

13 Y. Zhu, S. Murali, W. Cai, X. Li, J. W. Suk, J. R. Potts and R. S. Ruoff, *Adv. Mater.*, 2010, **22**, 3906–3924.

14 L. Chen, Y. Hernandez, X. Feng and K. Mullen, *Angew. Chem., Int. Ed.*, 2012, **51**, 7640–7654.

15 O. C. Compton and S. T. Nguyen, *Small*, 2010, **6**, 711–723.

16 K. P. Loh, Q. Bao, P. K. Ang and J. Yang, *J. Mater. Chem.*, 2010, **20**, 2277–2289.

17 T. Filleter, J. L. McChesney, A. Bostwick, E. Rotenberg, K. V. Emtsev, T. Seyller, K. Horn and R. Bennewitz, *Phys. Rev. Lett.*, 2009, **102**, 086102.

18 J. Zhang, W. Lu, J. M. Tour and J. Lou, *Appl. Phys. Lett.*, 2012, **101**, 123104.

19 D. R. Dreyer, S. Park, C. W. Bielawski and R. S. Ruoff, *Chem. Soc. Rev.*, 2010, **39**, 228–240.

20 J. Ou, J. Wang, S. Liu, B. Mu, J. Ren, H. Wang and S. Yang, *Langmuir*, 2010, **26**, 15830–15836.

21 J. Ou, Y. Wang, J. Wang, S. Liu, Z. Li and S. Yang, *J. Phys. Chem. C*, 2011, **115**, 10080–10086.

22 B. Bhushan, *Nanotribology and Nanomechanics*, 2008, p. 901.

23 C. Mu, H. Zhang, Y. Liu, Y. Song and P. Liu, *J. Rare Earths*, 2010, **28**, 43–47.

24 Q. Q. Shangguan and X. H. Cheng, *Wear*, 2007, **262**, 1419–1425.

25 D. Zhang, H. Fu, L. Shi, J. Fang and Q. Li, *J. Solid State Chem.*, 2007, **180**, 654–660.

26 X. Wang, N. Zhou, J. Yuan, W. Wang, Y. Tang, C. Lu, J. Zhang and J. Shen, *J. Mater. Chem.*, 2012, **22**, 1673.

27 Y. Guo, D. Wang, S. Liu and S. Wei, *Surf. Coat. Technol.*, 2011, **205**, 2924–2930.

28 M. S. S. Kobayashi, H. Kitagawa and W. W. L. Lam, *Chem. Rev.*, 2002, **102**, 2227–2302.

29 T. Bai and X. Cheng, *J. Rare Earths*, 2007, **25**, 114–119.

30 Q. Gu and X. Cheng, *Appl. Surf. Sci.*, 2007, **253**, 6800–6806.

31 D. A. Dikin, S. Stankovich, E. J. Zimney, R. D. Piner, G. H. B. Dommett, G. Evmenenko, S. B. T. Nguyen and R. S. Ruoff, *Nature*, 2007, **448**, 457–460.

32 D. Li, M. B. Müller, S. Gilje, R. B. Kaner and G. G. Wallace, *Nat. Nanotechnol.*, 2008, **3**, 101–105.

33 W. Hummers and R. Offeman, Preparation of graphitic oxide, *J. Am. Chem. Soc.*, 1958, **80**, 1339.

34 X. Sun, Z. Liu, K. Welsher, J. T. Robinson, A. Goodwin, S. Zaric and H. Dai, *Nano Res.*, 2008, **1**, 203–212.

35 H. Kang, A. Kulkarni, S. Stankovich, R. S. Ruoff and S. Baik, *Carbon*, 2009, **47**, 1520–1525.

36 S. Stankovich, D. A. Dikin, R. D. Piner, K. A. Kohlhaas, A. Kleinhammes, Y. Jia, Y. Wu, S. T. Nguyen and R. S. Ruoff, *Carbon*, 2007, **45**, 1558–1565.

37 H. Yang, F. Li, C. Shan, D. Han, Q. Zhang, L. Niu and A. Ivaska, *J. Mater. Chem.*, 2009, **19**, 4632–4638.

38 J. C. Meyer, A. K. Geim, M. I. Katsnelson, K. S. Novoselov, T. J. Booth and S. Roth, *Nature*, 2007, **446**, 60–63.

39 A. Fasolino, J. H. Los and M. I. Katsnelson, *Nat. Mater.*, 2007, **6**, 858–861.

40 C. Casiraghi, A. Hartschuh, E. Lidorikis, H. Qian, H. Harutyunyan, T. Gokus, K. S. Novoselov and A. C. Ferrari, *Nano Lett.*, 2007, **7**, 2711–2717.

41 S. Stankovich, D. A. Dikin, R. D. Piner, K. A. Kohlhaas, A. Kleinhammes, Y. Jia, Y. Wu, S. T. Nguyen and R. S. Ruoff, *Carbon*, 2007, **45**, 1558–1565.

42 S. Pei and H. M. Cheng, *Carbon*, 2012, **50**, 3210–3228.

43 J. Zhao, S. Pei, W. Ren, L. Gao and H. M. Cheng, *ACS Nano*, 2010, **4**, 5245–5252.

44 N. S. Tambe and B. Bhushan, *Nanotechnology*, 2005, **16**, 1549–1558.

45 D. G. Kurth and T. Bein, *Langmuir*, 1993, **9**, 2965–2973.

46 X. Cheng, Q. Gu and Y. Qi, *J. Rare Earths*, 2009, **27**, 711–716.

47 M. Golabek, M. Jurak, L. Holysz and E. Chibowski, *Colloids Surf., A*, 2011, **391**, 150–157.

48 A. Y. Fadeev and T. J. McCarthy, *Langmuir*, 1999, **15**, 3759–3766.

49 A. Quinn, H. Mantz, K. Jacobs, M. Bellion and L. Santen, *Europhys. Lett.*, 2008, **81**, 56003–56006.

50 B. Bhushan, *J. Vac. Sci. Technol., B: Microelectron. Nanometer Struct.–Process., Meas., Phenom.*, 2003, **21**, 2262.

51 Q. Gu and X. Cheng, *Surf. Coat. Technol.*, 2007, **202**, 126–132.

52 F. Gao, J. He, E. Wu, D. Liu, D. Yu, D. Li, S. Zhang and Y. Tian, *Phys. Rev. Lett.*, 2003, **91**, 015502.